NANO LETTERS

2005
Vol. 5, No. 11
2216−2219

Electronic Transport in Carbon Nanotubes with Random Coverage of Physisorbed Molecules

Sylvain Latil,[†,‡] Stephan Roche,[§] and Jean-Christophe Charlier*[,∥,⊥]

Department of Chemistry, University of Sussex, Falmer, BN1 9QJ Brighton, United Kingdom, Commissariat à l'Energie Atomique, DSM/DRFMC/SPSMS/GT, 17 rue des Martyrs, 38054 Grenoble Cedex 9, France, Unité de Physico-Chimie et de Physique des Matériaux (PCPM), Université Catholique de Louvain, Place Croix du Sud 1, B-1348 Louvain-La-Neuve, Belgium, and Research Center on Microscopic and Nanoscopic Electronic Devices and Materials (CERMIN), Université Catholique de Louvain, B-1348 Louvain-La-Neuve, Belgium

Received July 25, 2005

ABSTRACT

The chemical sensitivity of electronic transport in carbon nanotubes under the physisorption of molecular species is investigated using a tight-binding scheme, parametrized by first-principles calculations. Such a computational method enables tackling of the complex electronic properties of chemically grafted conducting nanotubes. Our calculations demonstrate that the impact of physisorption on the transport regime critically depends on the HOMO–LUMO gap of the attached molecules. In addition, the electronic mean free path exhibits a downscaling law with a lower dependence on the coverage density of grafted molecules than for conventional substitutional doping or homogeneous disorder.

The science of carbon nanotubes (CNTs) is a rapidly developing field due to the spectacular combination of molecular and mesoscopic scale phenomena and their relevance for both fundamental research and technological perspectives.[1] Nanotube-based electronics is probably one of the main potential uses of nanotubes. The elastic mean free path in metallic nanotubes is exceptionally long and further upscales with the diameter at a given disorder strength.[2,3] Transport measurements have confirmed quasi-ballistic transport using field effect transistors in the low bias regime.[4,5]

In addition, chemical sensing capabilities of carbon nanotube based devices appear very promising.[6,7] Indeed, functional groups can specifically be attached to the carbon nanotube surface either by physisorption[8] or by covalent bonding.[9,10] Conventional covalent functionalization significantly perturbs the atomic structure of the CNTs and its corresponding electronic properties. On the other hand, the physisorption of organic molecules on the nanotube sidewalls is an example of noncovalent functionalization involving π-stacking interactions and corresponding to a weaker binding energy.[11−15] The main interest in noncovalent functionalization stems from the negligible charge-transfer involved within the π-stacking interactions. The induced scattering is thus expected to be low and molecular dependent in opposition to the electrochemical covalent functionalization.[16] Consequently, a good knowledge of the CNT's reactivity and of the impact of the physisorption on the quantum transport is needed to guarantee their potential application as chemical sensors.

Recently, the effect of physisorption of small six-membered ring molecules C_6H_{2n} with $n = 3$, 4, 6, adsorbed onto the CNTs has been investigated experimentally, through thermopower measurements.[17] Such an approach indirectly addresses the effect of molecular physisorption on quantum transport since the thermopower can be related to the conductance modulations close to the Fermi level through the Mott formula.[18] However, to date, no theoretical works have accurately studied the issue of charge conduction properties in long carbon nanotubes with random coverage of physisorbed molecules.

In this paper, the effect of molecular physisorption on the diffusion mechanisms of metallic CNTs is theoretically investigated by combining first-principles calculations with reparametrized tight-binding (TB) models. The focus is made on the evaluation of the scattering strength, produced by a

[†] Department of Chemistry, University of Sussex.
[‡] Present address: Laboratoire de Physique du Solide, Facultés Universitaires Notre-Dame de la Paix, rue de Bruxelles 61, Namur, Belgium.
[§] Commissariat à l'Energie Atomique, DSM/DRFMC/SPSMS/GT.
[∥] Unité de Physico-Chimie et de Physique des Matériaux (PCPM), Université Catholique de Louvain.
[⊥] Research Center on Microscopic and Nanoscopic Electronic Devices and Materials (CERMIN), Université Catholique de Louvain.

10.1021/nl0514386 CCC: $30.25
Published on Web 10/07/2005

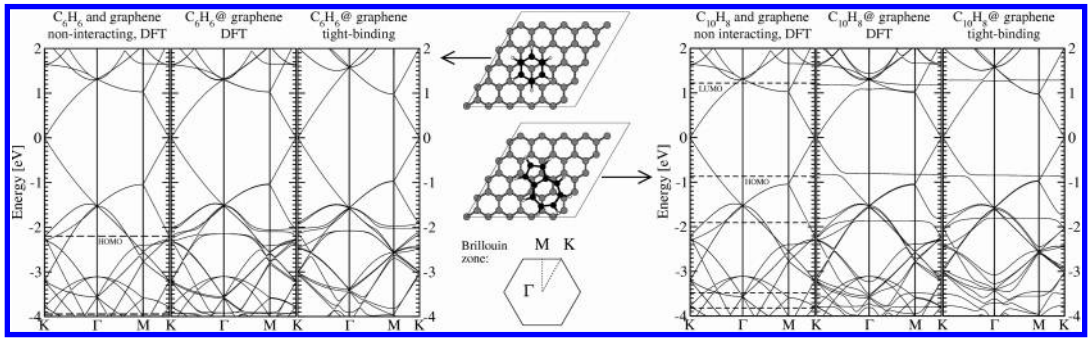

Figure 1. The electronic structures of a graphene 5 × 5 supercell with one adsorbed π-conjugated molecule. (left) the HOMO eigenstate of the isolated benzene (C_6H_6) molecule (shown with a dashed line in the left-hand frame) mixes up with the band structure of the graphene layer, to form a complex band structure (central frame). (right) an azulene ($C_{10}H_8$) molecule is physisorbed on the graphene sheet.

random coverage of π-conjugated hydrocarbon molecules (benzene (C_6H_6) and azulene ($C_{10}H_8$)) and acting on the wave packet propagation along the tube axis. The value of the HOMO−LUMO gap of the attached molecules and the energy of charge carriers are shown to be crucial parameters for determining the generic transport length scales (such as mean free path), and contribution of quantum interference effects, yielding weak localization. A combination of ab initio and semiempirical description of the system energetics is used to compute the transport coefficients in the Kubo formalism in real space.[19,20]

To adjust the parameters of the semiempirical Hamiltonian, and since the interaction between the CNT and each molecule is geometry-dependent, an ab initio study of the adsorption has been carried out prior to the TB analysis.[14,15] Assuming that the adsorption on a CNT or on graphene are equivalent, the atomic model is simplified when using a 5 × 5 graphene supercell with one adsorbed benzene or azulene molecule, instead of the cylindrical structure.

Electronic calculations have been performed on such system using the density functional theory within its local density approximation (LDA) to predict the optimal geometry and extract its electronic structure. The AIMPRO code[21] has been used, with standard norm-conserving pseudopotentials[22] and a 3 × 3 × 1 *k*-points sampling for the Brillouin zone integrations. The basis used is sufficient to obtain correct adsoption curves[14,15] (C atoms contain five s- and p-like and three d-like orbitals, and H atoms contain four s- and p-like orbitals).

From the optimized geometries[23] (displayed in the center of Figure 1), the LDA band structures are plotted for both isolated and interacting systems. The interaction acts as a mixing of the molecular single states with the underlying band structure, resulting in hybrid eigenstates, with low group velocity. However, due to the relatively large gaps of the isolated molecules (5.217 and 2.089 eV for benzene and azulene, respectively) only weak disturbance is induced around the Fermi energy, and the linear band dispersion is preserved.

Since the electronic properties of CNTs are well described by the so-called zone-folding model, a TB approach that safely neglects the weak effects of curvature is used.[1] The π-conjugated molecules are treated by the Hückel model.[24] Finally, the tight-binding Hamiltonian of the complete

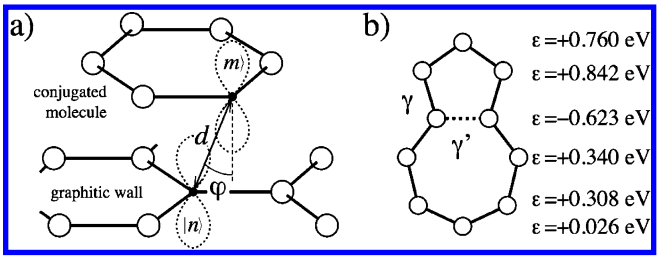

Figure 2. (a) Schematic view of the graphene−molecule interaction described by eq 2. The distance d and the angle φ are drawn. (b) The modified Hückel model for the azulene molecule. The on-site energies ϵ are corrected in order to account for the screening effect, while the hopping integrals are $\gamma = -2.63$ eV and $\gamma' = -2.08$ eV, respectively.

system, containing the interaction between CNT and N_{mol} molecules, reads

$$\hat{H} = \hat{H}_{CNT} + \sum_{M=1}^{N_{mol}} [\hat{H}_{mol}(M) + \hat{V}(M)] \qquad (1)$$

where $\hat{H}_{CNT}$ is the usual zone folding Hamiltonian, and $\hat{H}_{mol}(M)$ is the Hückel Hamiltonian related to the Mth molecule. The $\hat{V}(M)$ term in eq 1 corresponds to the interaction between the Mth molecule and the CNT and is expressed as follows

$$\hat{V}(M) = \sum_{n \in CNT} \sum_{m \in M} \beta \cos(\varphi) e^{(d-\delta)/l} |n\rangle\langle m| \qquad (2)$$

Such a coupling term was optimized to accurately reproduce the interaction between shells in a multiwalled CNT.[25] In eq 2, d corresponds to the distance between sites, while φ is the angle defined in Figure 2a. The parameters related to the interaction are $\delta = 3.34$ Å, $l = 0.45$ Å, and $\beta = -0.36$ eV.

The tight-binding parameters (on-site energies ϵ and hopping integrals γ) are adjusted to reproduce the band structure of a graphene sheet and the energy levels of isolated benzene and azulene molecules, calculated within LDA. A standard procedure has been used to set the parameters for the graphene or the CNT: $\epsilon_{CNT} = 0$ eV, $\gamma_{CNT} = -2.56$ eV, as well as for the benzene molecule: $\epsilon_{benz} = +0.411$ eV, $\gamma_{benz} = -2.61$ eV.

Due to an inhomogeneous charge distribution along the azulene molecule, the TB model has to be refined to properly account for screening effects. By adding an electrostatic correction, proportional to the net charge on each carbon atom (calculated with LDA), renormalized on-site energies for the azulene molecule have been deduced. The on-sites and the adjusted hopping integrals are given in Figure 2b. Within this approach, the TB value of the azulene HOMO−LUMO gap is 2.198 eV. Finally, the band structure computed with this modified TB model is compared to the previous ab initio results. As presented in Figure 1, this reparametrized semiempirical model gives an excellent description of the electronic states for both benzene and azulene adsorption cases.

The next step is the implementation of these parameters into an order $O(N)$ TB calculation to studying both the electronic structure (density of states) and the charge transport in a CNT with a random coverage of noncovalently attached molecules.[26] The computations of the conduction properties have been performed within the Kubo formalism using the linear response regime in real space.[19,20] This method consists of computing the energy-dependent diffusion coefficients of propagating electrons

$$D_{\mathrm{E}}(t) = \frac{Tr[(\hat{X}(t) - \hat{X}(0))^2\, \delta(E - \hat{H})]}{t\, Tr[\delta(E - \hat{H})]} \qquad (3)$$

whose time dependence fully determines the transport mechanism and the typical elastic transport length scale (mean free path).

In eq 3, $\hat{X}(t)$ is the Heisenberg representation of the position operator along the nanotube axis and $Tr[\delta(E - H)] = n(E)$ is the normalized density of states. The computations of the traces are performed in real space, using an order $O(N)$ recursion technique,[19,20] that has been successfully implemented to investigate the boron and nitrogen doping in carbon nanotubes.[27]

The density of states (DOS) of a (10,10) carbon nanotube, with random coverage of adsorbed molecules is calculated within this framework. Figure 3a presents the DOS for a nanotube with benzene coverage density of 16.3% (such density corresponds to the ratio of adsorbed mass of the molecule over CNT mass) whereas Figure 3b illustrates the DOS for the nanotube with azulene coverage density of 11.5%.

Since the coupling intensity is weak, the DOS plotted in Figure 3 displays the reminiscent discrete molecular levels, slightly enlarged by the mixing with the underlying continuum of π or π^* bands. Peaks arising from molecular HOMO and LUMO levels are labeled.

In the case of the benzene adsorption, the DOS is weakly affected at charge neutrality point, and the computed diffusion coefficient shows almost no deviation from the linear scaling in time (ballistic regime). Elastic backscattering induced by benzene molecules is thus vanishingly low at Fermi level (Figure 3c) and does not produce sufficient deviation to determine an elastic mean free path below $\sim$100 μm.

In contrast, in the case of azulene molecules, the HOMO level is located in the close vicinity of the last occupied Van

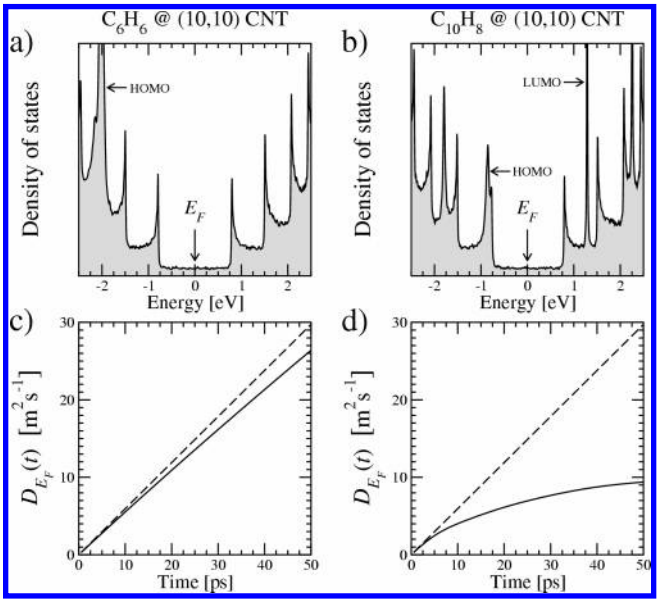

Figure 3. (a) DOS of the (10,10) CNT with a C_6H_6 density coverage of 16.3%. The HOMO molecular state is located by an arrow. (b) Same as in (a) but for a $C_{10}H_8$ density coverage of 11.5%. HOMO and LUMO levels are identified by arrows. (c) Time-dependent diffusion coefficient (at Fermi level) for the C_6H_6@CNT system, showing quasi-ballistic behavior (solid line). Ballistic conduction for the pristine CNT case is also reported (dashed line). (d) Time-dependent diffusion coefficient for the $C_{10}H_8$@CNT structure, showing saturation at large times (diffusive regime).

Hove singularity of the CNT. Although the total DOS remains basically unaffected around the Fermi energy, the azulene adsorption turns out to impact more significantly on the intrinsic electronic current. Indeed, as shown in Figure 3d, the diffusion coefficients of propagating electrons at the Fermi level depart more strongly from the ballistic regime.

The nonlinear time dependence of $D_{\mathrm{E}}(t)$ allows extraction of the elastic relaxation time τ and, knowing the Fermi velocity v_{F}, the corresponding electronic mean free path l_{e}. Figure 4 presents the evolution of the elastic mean free path as a function of the azulene coverage density, at the Fermi level (charge neutrality point) and for an energy closer to the HOMO resonance ($E = -0.2\gamma_0 \simeq -0.54$ eV).

The energy-dependent behaviors for two different coverages of 2% and 25% are shown in the inset of Figure 4. At the charge neutrality point, such an increase of coverage density yields a decrease of l_{e} by a factor of 3. Such downscaling is found to be much slower than expected from a conventional Fermi golden rule (FGR).[2,3] Indeed, in contrast, the effect of substitutional chemical impurities investigated within the FGR approach[27] was shown to produce a linear decreasing of l_{e} with the impurity density. Different from substitutional impurities, in the case of physisorption, the underlying carbon lattice is only disturbed as a second-order process, and as confirmed by our numerical results, corresponding backscattering behavior turns out to be much weaker.

Another remarkable feature is the strong asymmetry of backscattering with respect to the charge neutrality point. Indeed, the effect of the molecules on transport is much more pronounced in the vicinity of the HOMO resonance for which

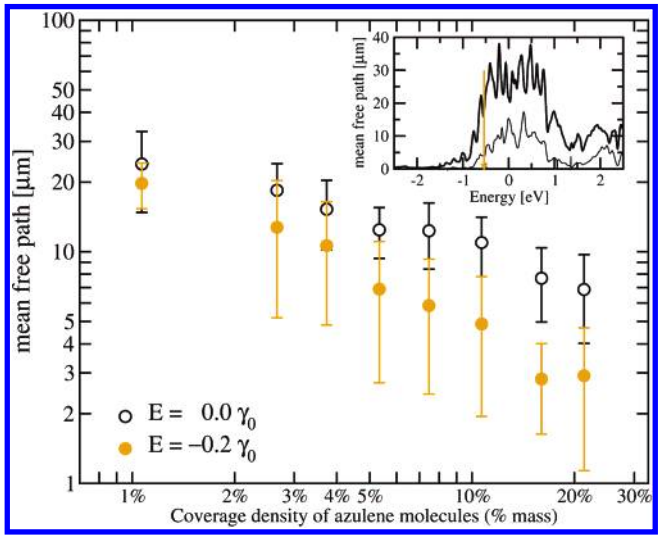

Figure 4. Electronic mean free path of a $C_{10}H_8$@CNT nanostructure versus the density of physisorbed molecules ρ_{mol} and for two different Fermi level positions. The origin of the error bars is the expectation of the traces in eq 3. (inset) Energy-dependence of l_e for $\rho_{mol} = 2\%$ (bold curve) and $\rho_{mol} = 25\%$ (solid curve).

we estimate (Figure 4, inset) a mean free path in the nanometer range. The main part of Figure 4 shows the downscaling law for l_e at two chosen energies. For $E = -0.2\gamma_0$, the mean free path is roughly divided by a factor of 6 for a coverage increase of ~20%. At low coverage the initial values of l_e for both energies are similar, but the downscaling of l_e with respect to the impurity coverage density turns out to be different. This remarkable feature demonstrates the unconventional effect of physisorption on the scaling behaviors of the elastic length scales.

In the diffusive regime, it is possible to estimate the relative conductance change upon Fermi level shift. Indeed, the conductance scales linearly with l_e, so that the ratio of the conductance at two different energies is related to the inverse ratio of corresponding mean free paths. For instance, comparing the situation of a Fermi level at HOMO resonance with the charge neutrality point one gets

$$G(E_F \sim \epsilon_{HOMO}) = l_e(E_F \sim \epsilon_{HOMO})/l_e(E_F=0)G(E_F=0) \quad (4)$$

so that a quantitative measure of conductance changes upon Fermi level shift is possible.

In conclusion, physisorption effects on electronic conduction have been shown to critically depend on the nature of molecular species and their HOMO−LUMO gap positioning with respect to the Fermi level. Benzene molecules yield vanishing modulations of the intrinsic conductance, whereas azulene molecules (with HOMO−LUMO gap of about ~2.07 eV) produce substantial elastic backscattering in the nanotube, resulting in mean free paths on the order of a few micrometers for large coverage. Other small gap π-conjugated hydrocarbon molecules such as fulvene should yield similar effects. Such a possibility of creating/removing a reversible elastic disorder by a simple adsorption/desorption of molecules covering the nanotube surface opens interesting perspectives for experimental studies and potential applications in nanotechnology.

Acknowledgment. S.L. acknowledges financial support from the European Community through its IHP program "new fullerene-like materials". J.-C.C. acknowledges the FNRS of Belgium for financial support. Part of this work is supported by the Belgian Program on Interuniversity Attraction Poles (PAI5/1/1), to the ARC sponsored by the Communauté Française de Belgique, NANOQUANTA and FAME Networks of Excellence. S.R. acknowledges ACI grants Transnanofils and No. NR044 "NOCIEL".

References

(1) Saito, R.; Dresselhaus, G.; Dresselhaus, M. S. *Physical Properties of Carbon Nanotubes*; Imperial College Press: London, 1998.
(2) White, C. T.; Todorov, T. N. *Nature* **1998**, *393*, 240−242.
(3) Triozon, F.; Roche S.; Rubio, A.; Mayou, D. *Phys. Rev. B* **2004**, *69*, 121410.
(4) Derycke, V.; Martel, R.; Appenzeller, J.; Avouris, P. *Nano Lett.* **2001**, *1* 453−456.
(5) Javey, A.; Guo, J.; Wang, Q.; Lundstrom, M.; Dai, H. J. *Nature* **2003**, *424*, 654−657.
(6) Star, A.; Han, T. R.; Gabriel, J. C.; Bradley, K.; Gruner, G. *Nanolett.* **2003**, *3*, 1421−1423.
(7) Balasubramanian, K.; Sordan, R.; Burghard, M.; Kern, K. *Nano Lett.* **2004**, *4*, 827−830.
(8) Star, A.; Liu, Y.; Grant, K.; Ridvan, L.; Stoddart, J. F.; Steuerman, D. W.; Diehl, M. R.; Boukai, A.; Heath, J. R. *Macromolecules* **2003**, *36*, 553−560.
(9) Bahr, J. L.; Yang, J. P.; Kosynkin, D. V.; Bronikowski, M. J.; Smalley, R. E.; Tour, J. M. *J. Am. Chem.* Soc. **2001**, *123*, 6536−6542.
(10) Zhu, W.; Minami, N.; Kazaoui, S.; Kim, Y. *J. Mater. Chem.* **2004**, *14*, 1924−1926.
(11) Zhao, J.; Lu, J. P.; Han, J.; Yang, C. K. *Appl. Phys. Lett.* **2003**, *82*, 3746−3748.
(12) Giannozzi, P. *Appl. Phys. Lett.* **2003**, *84*, 3936−3937.
(13) Arab, M.; Picaud, F.; Devel, M.; Ramseyer, C.; Girardet, C. *Phys. Rev. B* **2004**, *69*, 165401.
(14) Tournus, F.; Charlier, J.-C. *Phys. Rev. B* **2005**, *71*, 165421.
(15) Tournus, F.; Latil, S.; Heggie, M. I.; Charlier, J.-C. *Phys. Rev. B* **2005**, *72*, 075431.
(16) Balasubramanian, K.; Burghard, M. *Small* **2005**, *1* (No. 2), 180−192.
(17) Sumanasekera, G. U.; Pradhan, B. K.; Romero, H. E.; Adu, K. W.; Eklund, P. C. *Phys. Rev. Lett.* **2002**, *89*, 166801.
(18) Small, J. P.; Perez, K. M.; Kim, P. *Phys. Rev. Lett.* **2003**, *91*, 256801.
(19) Roche, S. *Phys. Rev. B* **1999**, *59*, 2284−2291.
(20) Roche, S.; Saito, R. *Phys. Rev. Lett.* **2001**, *87*, 246803.
(21) Briddon, P. R.; Jones, R. *Phys. Status Solidi B* **2000**, *217*, 131−171.
(22) Bachelet, G. B.; Hamann, D. R.; Schlüter, M. *Phys. Rev. B* **1982**, *26*, 4199−4228.
(23) Equilibrium distances (energies of adsorption) are found to be 3.25 Å (25.1 kJ·mol^{-1}) for the benzene and 3.28 Å (37.6 kJ·mol^{-1}) for the azulene molecules.
(24) Salem, L. *The Molecular-Orbital theory of π-conjugated systems*; Benjamin: Reading, MA, 1966.
(25) Lambin, Ph.; Meunier, V.; Rubio, A. *Phys. Rev. B* **2000**, *62*, 5129−5135.
(26) Besides the random distribution, the molecules are always stacked as shown in Figure 1. The azulene molecule is assumed to be aligned with the tube axis, and no mutual molecular interactions were taken into account when generating the grafted nanostructures.
(27) Latil, S.; Roche, S.; Mayou, D.; Charlier, J.-C. *Phys. Rev. Lett.* **2004**, *92*, 256805.

NL0514386